



A method for improving the seismic performance of RC moment frame buildings

O. Arroyo⁽¹⁾, and S. Gutiérrez⁽²⁾

⁽¹⁾ Doctoral Candidate, Departamento de Ingeniería Estructural y Geotecnia, Pontificia Universidad Católica de Chile, odarroyo@uc.cl

⁽²⁾ Associate Professor, Departamento de Ingeniería Estructural y Geotecnia, Pontificia Universidad Católica de Chile, sgutierr@ing.puc.cl

Abstract

An optimization approach to determine the column and beam dimensions that optimize the seismic performance of a given RC Moment Frame building is introduced. The approach is based on eigenfrequency optimization using homogenization and it leads to the introduction of a highly efficient computational algorithm, which can run in consumer-level computers and obtain results within minutes. A detailed example is provided for a 10 story building, whose seismic performance is analyzed in OpenSees using pushover and nonlinear response history analysis. The results show that, when compared with the traditional design which has columns and beams of uniform dimensions between stories, the overstrength and ductility are increased by 26% and 90%, respectively. Furthermore, the median results of the Nonlinear Time History Analysis show that interstory drifts have important reductions for the first six floors of the building, while in the four upper floors they increase only slightly. All these improvements are achieved without increasing the amount of material consumption, since the optimized building is constrained to use the same volume of concrete used in the traditional design.

Keywords: structural optimization, topology optimization, reinforced concrete moment frames, seismic performance,

1. Introduction

Several seismic optimization methods for RC structures have been proposed based on a variety of formulations [1] and different optimization approaches [2, 3, 4, 5]. Despite their ability to achieve good results, these methods have two major downsides: they are computationally expensive and their optimization algorithms may experience issues with the convergence and numerical instability. In order to overcome these limitations, researchers have proposed strategies [6, 7, 8] that have shown improvements on these areas; however, there is still room for innovation and new ideas on this research field. In this paper, we introduce a new formulation for the seismic optimization of RC structures. We began with a reformulation of the seismic optimization problem, by setting as objective function the maximization of the first eigenfrequency (ω) of the structure; meanwhile, code provisions and the structural cost are considered as the optimization constraints. The rationale for maximizing the first eigenfrequency is that it ensures the best performance in the elastic regime of the building and delays the start of the inelastic range.

This formulation has important advantages. First, it directly optimizes an important property of the structure with significant influence on its seismic behavior. In addition to this, it allows to use a strong mathematical theory [9, 10, 11, 12, 13, 14] to find an optimality criteria and formulate an optimization algorithm with outstanding numerical e

fficiency and mathematical formulation and computational algorithm for the maximization of the first eigenfrequency. Section 3 provides a detailed application of the proposed methodology for a 10-story building. Section 4 shows a performance comparison of the optimum building against a non-optimized one by means of pushover analysis and a nonlinear response history analysis based on the ground motion suite of the FEMA P695. Finally, section 5 presents the conclusions of this study.



2. Optimization based on full homogenization

Now we briefly describe the mathematical basis of the full homogenization method. A more complete description of the method can be found in [10] and, more specifically, for eigenfrequency optimization in [15].

2.1. Mathematical model

Eigenfrequency optimization is formulated using PDEs as follows:

$$\begin{aligned}
 & \text{Max} && \omega_n(\boldsymbol{\rho}) \\
 & \text{subject to} && \boldsymbol{\rho} \geq \boldsymbol{\rho}_{\min} \\
 & && V(\boldsymbol{\rho}) = V_0 \\
 & && -\text{div}(C\boldsymbol{e}(u)) = \omega_n^2 \boldsymbol{\rho} u \quad \text{in } \Omega \\
 & && C\boldsymbol{e}(u)n = 0 \quad \text{on } \Gamma_N \\
 & && u = 0 \quad \text{on } \Gamma_D
 \end{aligned} \quad (1)$$

Here, $\boldsymbol{\rho}$ represents density of material, which should be greater than a function $\boldsymbol{\rho}_{\min}$ in the domain Ω , and $V(\boldsymbol{\rho}) = V_0$ means that the total amount of material must be equal to a predefined volume V_0 . The third constraint means that ω_n is an eigenfrequency of the structure, while the fourth and fifth represent the boundary conditions for the building.

As a result of using the material density $\boldsymbol{\rho}$ as the optimization variable, this formulation requires $\boldsymbol{\rho}_{\min}$ and Ω to be defined in terms of the lower and upper bounds of the dimensions of the structural members. Once the optimal density of material $\boldsymbol{\rho}_{opt}$ has been obtained, it needs to be expressed as column and beam dimensions. The steel reinforcement to be used is calculated after the optimization.

Let $\Omega \subset \mathbb{R}^2$ be a bounded open set in \mathbb{R}^2 . In Ω we have two linearly elastic materials with Hooke's laws A and B . Let δ be a positive real number, $\delta \approx 0$, such that $A = \delta B$. Therefore, A is the Hooke law of a very flexible material, and in the limit when $\delta \rightarrow 0$, it imitates void. Let $\chi \in L^\infty(\Omega; \{0,1\})$ be a characteristic function of the most rigid material, i.e., $\chi(x) = 1$ if material B is present at x , and $\chi(x) = 0$ otherwise.

The heterogeneous Hooke's law in Ω is

$$C(x) = (1 - \chi(x))A + \chi(x)B.$$

The heterogeneous density in Ω is

$$\rho(x) = (1 - \chi(x))\rho_A + \chi(x)\rho_B,$$

where $\rho_A, \rho_B > 0$ are the densities of the materials.

The boundary $\partial\Omega$ is divided in two disjoint parts Γ_D and Γ_N supporting respectively Dirichlet boundary condition (zero displacement) and Neumann boundary condition (zero traction). The vibration frequencies ω of the heterogeneous domain Ω , filled by A and B , are the square roots of the eigenvalues of the following problem:



$$\begin{aligned} -\operatorname{div}(Ce(u)) &= \omega^2 \rho u & \text{in } \Omega \\ Ce(u)n &= 0 & \text{on } \Gamma_N \\ u &= 0 & \text{on } \Gamma_D \end{aligned} \quad (2)$$

where $u \in H^1(\Omega)^2$ is the displacement field, and $e(u) = \frac{1}{2}(\nabla u + \nabla^T u)$ is the infinitesimal strain tensor.

As is well known, problem (3) admits a countable family of positive eigenvalues.

$$0 < \omega_1^2 \leq \omega_2^2 \leq \dots \leq \omega_k^2 \rightarrow +\infty$$

In this work we want to maximize the first eigenvalue, which is given by the following formula

$$\omega_1^2 = \min_{u \in H} \frac{\int_{\Omega} Ce(u) : e(u) dx}{\int_{\Omega} \rho |u|^2 dx},$$

where $H = \{u \in H^1(\Omega)^2 | u = 0 \text{ on } \Gamma_D\}$.

We want to find the best arrangement of A and B in Ω that maximizes ω_1^2 . If $\rho_A = \rho_B$ and there is no volume constraint on the amount being used of each material, the problem has a trivial solution, that is to fill Ω only with the most rigid material, namely, that with elasticity tensor B . Therefore, we add a constraint on the volume being used of that material, say V_0 , and introduce a Lagrange multiplier $l \in R$ for such constraint. Then the optimization problem becomes

$$\sup_{\chi \in L^\infty(\Omega; \{0,1\})} \left\{ \omega_1^2 + l \left(\int_{\Omega} \chi(x) dx - V_0 \right) \right\} \quad (3)$$

We want to find a sequence of characteristic functions χ_n that maximizes (4). However, it is known that this problem admits no optimal solution. Hence, one needs to enlarge the class of admissible designs by allowing fine mixtures of the two materials on a scale which is much smaller than the mesh used for the actual computation. However, the set of all Hooke's laws that can be created is not known. Fortunately in the case of eigenfrequency optimization, the optimal microstructure is known to be among the subset of sequential laminates [26]. This process of enlarging the set of admissible designs in order to get a well-posed problem is called relaxation. The derivation of the relaxed formulation was done by the pioneering work of Murat and Tartar [28], which is briefly sketched for the sake of completeness.

Let $\chi_n \in L^\infty(\Omega; \{0,1\})$ be a maximizing sequence for (4). We want to pass to the limit in (4) and compute its maximal value. The sequence χ_n is bounded in $L^\infty(\Omega; \{0,1\})$, therefore one can extract a subsequence, still denoted by χ_n , such that it converges in $L^\infty(\Omega)$ weak- \check{a} to θ . The limit θ is, in general, a density, i.e., it belongs to $L^\infty(\Omega; [0,1])$. According to the theory of H-convergence [14], a subsequence of $C_n = (1 - \chi_n(x))A + \chi_n(x)B$ H-converges to a homogenized Hooke's law C^* as $n \rightarrow \infty$. As a consequence the eigenvalue $(\omega_1^n)^2$ and its corresponding normalized eigenfunction u_1^n , solutions to

$$\begin{aligned} -\operatorname{div}(C_n e(u)) &= (\omega_1^n)^2 \rho_n u & \text{in } \Omega \\ C_n e(u)n &= 0 & \text{on } \Gamma_N \\ u &= 0 & \text{on } \Gamma_D \end{aligned} \quad (4)$$



satisfy $\lim_{n \rightarrow \infty} \omega_1^n = \omega_1$, and the sequence of eigenfunctions u_1^n converges weakly in $H^1(\Omega)^2$ and strongly in $L^2(\Omega)^2$ to a limit eigenfunction u_1 such that

$$\begin{aligned} -\operatorname{div}(C^* e(u_1)) &= \omega_1^2 \bar{\rho} u_1 & \text{in } \Omega \\ C^* e(u_1) n &= 0 & \text{on } \Gamma_N \\ u_1 &= 0 & \text{on } \Gamma_D \end{aligned} \quad (5)$$

with $\bar{\rho}(x)$, the weak limit of the sequence ρ_n , *i.e.*,

$$\bar{\rho}(x) = (1 - \theta(x))\rho_A + \theta(x)\rho_B.$$

In turn C^* belongs to \mathbf{G}_θ , defined as

$$\mathbf{G}_\theta = \{ \text{H-limits of } C_n = (1 - \chi_n)A + \chi_n B \mid \chi_n \square \theta \}$$

Thanks to the work of Murat and Tartar [14], we can find the optimal Hooke's law C^* in the subset L_θ of sequential laminates obtained by laminating B around a core of A in proportion θ and $1 - \theta$, respectively.

Thus, we define a relaxed objective functional by

$$\max_{\theta \in L^\infty(\Omega; [0,1])} \max_{C^* \in L_\theta} \left\{ \omega_1^2(\theta, C^*) + l \left(\int_\Omega \theta(x) dx - V_0 \right) \right\} \quad (6)$$

The new material is built by laminating, in a very fine scale, a proportion θ_1 of B with a proportion $1 - \theta_1$ of A in one direction, say e^1 , and then the resultant tensor A^1 is laminated again, at a scale coarser than the previous one but still finer than the macroscale, in a direction e^2 , and in proportion θ_2 with one of the initial materials, say A , and obtain C^* , the Hooke's law of a rank 2 laminate. Figure 1 illustrates this procedure.

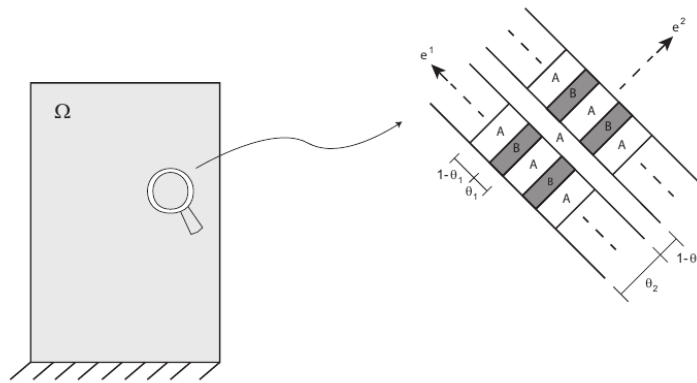


Figure 1 - Homogenized rank 2 laminated material

The effective Hooke's law C^* is obtained from equation (2.68) in [10]

$$C^* = B + (1 - \theta) \left((A - B)^{-1} + \theta (m_1 f_B(e^1) + m_2 f_B(e^2)) \right)^{-1} \quad (7)$$



Where $\theta = \theta_1 \theta_2$ is the total proportion of material B , the unit vectors e^1, e^2 are the lamination directions, the real numbers $0 \leq m_1, m_2 \leq 1$ such that $m_1 + m_2 = 1$, are the lamination parameters, and $f_B(e^i)$ is a positive non-definite fourth-order tensor defined for any symmetric matrix ξ by the following quadratic form

$$f_B(e^i)\xi : \xi = \frac{1}{\mu} |\xi e^i|^2 - K (\xi e^i \cdot e^i)^2,$$

where $K = \frac{\mu + \lambda}{\mu(2\mu + \lambda)}$ and μ, λ are the Lamé parameters of material B .

2.2. Optimality criteria method

By means of theorem (4.1.46) in [27], in the case when the first eigenvalue is simple we can find the optimal lamination parameters and lamination directions in order to maximize our objective function.

If the eigenvalues of the stress tensor $\sigma = C^* e(u_1)$ are denoted σ_1 and σ_2 , they are given by

$$\sigma_1 = \frac{1}{2} \left(\sigma_{11} + \sigma_{22} + \sqrt{(\sigma_{11} - \sigma_{22})^2 + 4\sigma_{12}^2} \right),$$

$$\sigma_2 = \frac{1}{2} \left(\sigma_{11} + \sigma_{22} - \sqrt{(\sigma_{11} - \sigma_{22})^2 + 4\sigma_{12}^2} \right)$$

The lamination parameters are

$$m_1 = \frac{|\sigma_2|}{|\sigma_1| + |\sigma_2|} \quad \text{and} \quad m_2 = \frac{|\sigma_1|}{|\sigma_1| + |\sigma_2|},$$

therefore the intermediate proportions are:

$$\theta_1 = \frac{|\sigma_1| + \theta |\sigma_2|}{|\sigma_1| + |\sigma_2|} \quad \theta_2 = \frac{\theta (|\sigma_1| + |\sigma_2|)}{|\sigma_1| + \theta |\sigma_2|}.$$

The lamination directions are chosen as the eigenvectors of σ . Then

$$e^1 = \begin{pmatrix} \frac{\sigma_{12}}{\sqrt{\sigma_{12}^2 + (\sigma_1 - \sigma_{11})^2 + \delta^2}} \\ \frac{\sigma_1 - \sigma_{11}}{\sqrt{\sigma_{12}^2 + (\sigma_1 - \sigma_{11})^2 + \delta^2}} \end{pmatrix} \quad e^2 = \begin{pmatrix} e_y^1 \\ -e_x^1 \end{pmatrix},$$

where $\delta = \varepsilon 10^{-6}$ is introduced to avoid numerical problems.

The optimal density of rigid material is chosen by:

$$\theta = \max \left\{ \theta_{min}, \min \left\{ 1, \sqrt{\frac{g^*(\sigma)}{l \int_{\Omega} \bar{\rho} |u|^2}} \right\} \right\} \quad (8)$$

where:



θ_{min} = lower limit for material density.

$$g^*(\sigma) = \frac{2\mu + \lambda}{4\mu(\mu + \lambda)} (|\sigma_1| + |\sigma_2|)^2$$

l = lagrange multiplier for the volume constraint of the rigid material

$$\bar{\rho} = \theta_p B + (1 - \theta_p) A$$

θ_p = optimal density of rigid material obtained in the previous iteration

u = first eigenfunction obtained in the previous iteration.

2.3. Computational algorithm

The previous subsection shows the formulas necessary to implement a computational algorithm. The algorithm is constructed as follows:

1. Initialization of the design parameters (θ_0, C_0^*) .
2. Iteration until convergence, for $k \geq 0$:
 - a) Compute the first eigenfunction u_1^k with the previous design parameters (θ_k, C_k^*) , and calculate the stress field σ_k .
 - b) Update the design variables $(\theta_{k+1}, C_{k+1}^*)$ by using the stress σ_k in the explicit optimality formulas (8) and (9).

To optimize 3D buildings, this algorithm is applied to frames in each building direction X and Y independently, because it is expected that for structures without important irregularities, the first mode in each direction is not significantly affected by the first mode in the perpendicular direction.

3. Optimization of a 10 story building

In order to demonstrate the proposed method, we consider a 10 story building whose plan view is shown in figure 2. The building has four moment resisting frames in the X direction and seven in the Y direction, it is completely regular and its total height are 30m. In order to establish a baseline for comparison, this building is designed using ETABS v13.1.2 for residential purposes according to the ACI 318-11[16] for the state of California, using soil type D conditions, $S_a = 1.0g$ and a 2% drift limit and considering $f_c = 28MPa$ and $F_y = 420MPa$

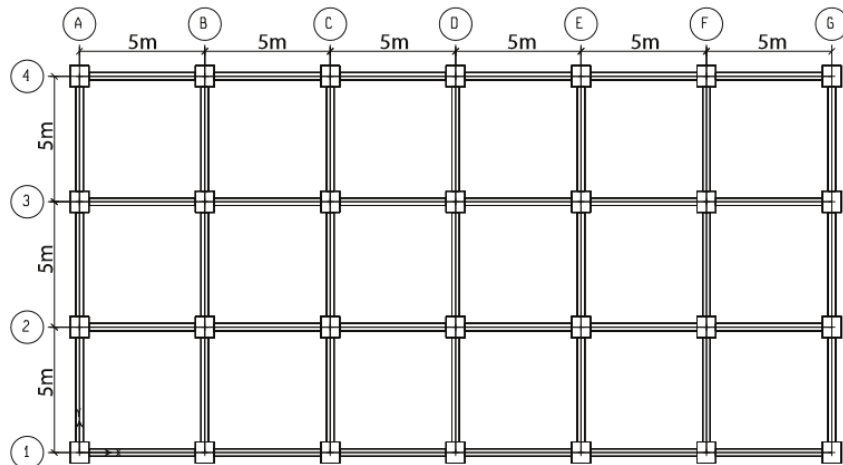


Figure 2 – Plan view of the 10 story building



The design requirements of this code are fulfilled using columns with a cross section of 55cm x 75cm and a reinforcement ratio of 1.2%. Beam sections are calculated and sections of 30cm x 40cm with a top and bottom reinforcement of 3 ϕ 3/4in with an additional ϕ 3/4in for top reinforcement in the BC joints are found to satisfy the code requirements. As a consequence of its regularity, this building can be optimized independently in each direction. First, we will proceed with the X direction. The first step is to define the optimization domain Ω . We begin by establishing a centerline consistent with the elevation view of a typical moment resisting frame of this direction, i.e. those in axis 1 to 4. After that, we set the maximum dimension for columns and beams, which are used to define the domain borders from the centerline. In this case, 80cm are chosen for the maximum column dimension in the X direction, and 50cm for the beams. It is noteworthy that due to its domain definition, this optimization method does not allow to include the beams width. The second step is to define the value of V_0 . This can be done using different approaches, for instance, economic considerations together with engineering criteria based on experience with similar projects. Taking into account that Ω is a bidimensional domain, V_0 is defined as a fraction of the area of Ω . For this example, and for the sake of making a fair comparison, this limit is set as the area of an elevation of the baseline building in the optimization direction, i.e. the area of its elevation view in this direction, which corresponds to a 76% of the domain area. By doing this, we are ensuring that the optimized building uses the same volume as the baseline.

A third step involves defining the minimum column and beam dimensions, so that code requirements regarding this issue are fulfilled. Several approaches can be used for this, for example, by performing an approximate analysis of the structure, calculating axial loads for columns and bending moments in the BC joints and finding a lower limit for dimensions so that the building can withstand such forces. Once this limit has been set, it is expressed as the minimum density of material θ_{min} . Let be noted that the advantage of the algorithm is that θ_{min} can be set as a function in the domain Ω , therefore, minimum dimension can be set independently for different elements of the building. In this example, 50cm are considered as the minimum column dimension and 30cm for the beams. The algorithm described in section 2 is implemented in FreeFem++ [17] and the optimization results are shown in figure 3. Here, the optimization result is the material density θ , which is converted into the dimension of the structural elements by integrating over its corresponding area.

To perform the optimization in the Y direction, we follow the same steps. First we select the maximum dimensions for columns and beams as 85cm and 50cm, respectively. After that, we calculate V_0 as the 85% of the domain and finally, we consider that the minimum dimension for columns are 60cm, while for beams we have 30cm. The optimization results are shown in figure 4 with the corresponding rounded dimensions in cm next to each element. Based on the dimensions calculated for both directions, the optimized building is designed in ETABS v13.1.2 for the same loading cases as the traditional one. The design results indicate that the elements of the optimized building use the same reinforcement ratios as their traditional counterparts, therefore, both buildings will have the same amount of concrete and reinforcing steel. The resulting dimensions of elements rounded to multiples of 5cm are shown in table 1. From a construction perspective, the optimized building would require a higher level of supervision, especially in order to ascertain that the column dimensions correspond to the ones resulting from the optimization. Although beams also change between stories, since their depth remains constant within a story level, it does not require special considerations for their construction. The additional supervision required certainly increases the construction costs, however, the benefits in seismic performance (shown in the next section) do compensate these costs.

Table 1. Dimensions for 10-story buildings (all dimensions are given in cm)

	Optimized building				Traditional building	
	Columns		Beams		Columns	Beams
Story	Inner	Outer	X Dir	Y Dir	Both	Both
10	50x60	50x60	35x35	35x35	55x75	35x40
9	55x65	55x65	35x35	35x35	55x75	35x40



8	55x70	55x70	35x40	35x40	55x75	35x40
7	60x70	55x70	35x40	35x40	55x75	35x40
6	60x75	55x75	35x40	35x40	55x75	35x40
5	60x75	55x75	35x40	35x40	55x75	35x40
4	65x80	60x80	35x45	35x45	55x75	35x40
3	70x80	65x80	35x45	35x50	55x75	35x40
2	70x80	70x80	35x45	35x50	55x75	35x40
1	70x85	70x80	35x45	35x45	55x75	35x40

An important remark about the optimization algorithm is its outstanding numerical efficiency. Running the optimization on a laptop with an Intel Core i5 4200U at 1.6GHz and 4GB of RAM, it takes 1508.76 seconds to run the optimization for both directions. In the following section, we compare the performance of the optimized and the baseline buildings.

4. Structural performance of the optimized building

In order to have a comprehensive vision of the structural behavior, OpenSees [18] is used to perform a 2D Pushover Analysis for the typical X and Y frames of the buildings, i.e. frames corresponding to elevations designated by B and 2 in figure 2. Based on these results, ductility (μ) and overstrength (Ω_0) are calculated according to the FEMA P695 [19] methodology. We also perform a Nonlinear Time History Analysis for the two buildings using the 44 ground motion suite of the FEMA P695, properly normalized and anchored such that the median of the spectral acceleration set matches the spectral acceleration of the Dmax spectrum at the fundamental period of the buildings. After this process, the suite was ran at three different scale factors, 1.0, 2.2 and 3.5 and the displacement and interstory drift were recorded for each story of the building. For each scale factor we calculate the median of the maximum values taken from each record of the GM suite, for each story of the building and each demand parameter, i.e., displacement and drift.

The mathematical model of the structure is created using force-based elements with confined and unconfined concrete. To avoid localization issues we use the Constant Fracture Energy Criterion [20] with $G_c = 180\text{N/mm}$; with concrete properties $f_c = 28\text{MPa}$, $f_{cc} = 31\text{MPa}$, $\epsilon_c = 0.0019$ and $\epsilon_{cc} = 0.0028$. Reinforcing steel is modelled using $E_s = 210\text{GPa}$, $f_y = 420\text{MPa}$, $f_u = 630\text{MPa}$ and an ultimate strain $\epsilon_u = 0.14$. P-Delta effects are included and a displacement control is used in the Pushover using 0.5mm steps. Mode shapes and elastic behavior are checked and found to be consistent with the expected behavior. A uniform gravitational load $w = 3.5\text{tonf/m}$ is applied to beams, and point loads are applied to nodes to account for the self-weight of columns. Masses were assigned in nodes based on the tributary areas and the elements self-mass.

Pushover Results for the X and Y directions are shown in figure 3 and they show that the optimized building performs significantly better than the baseline in several aspects:

- The slope in the elastic range is steeper for the optimized building, which means that it is more rigid than the traditional. This comes as a direct consequence of the optimization, as its goal is maximizing the first eigenvalue of the building.
- The maximum base shear V_{\max} supported by the optimized building is higher than the one from the baseline. This could have an important practical implication, as it suggests that the optimized building could withstand earthquakes with higher accelerations before starting to deteriorate.
- The optimized building has a smaller post-peak slope than baseline, hence its performance is better in this range because it deteriorates at a slower rate.

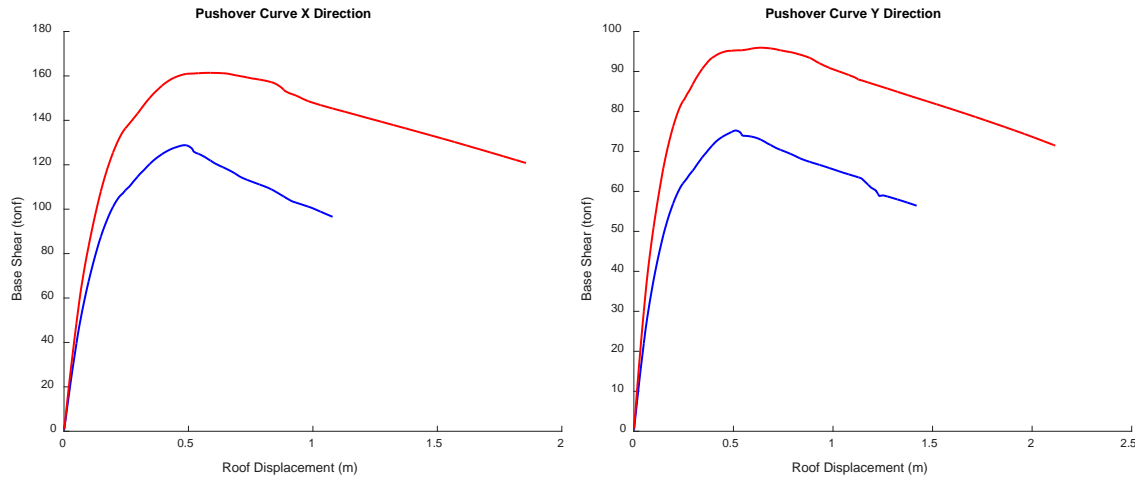


Figure 3 – Pushover results

This analysis is further confirmed by calculating the overstrength (Ω_0) and ductility (μ) as shown in table 2, where it can be observed that the optimized building has an overstrength that is 23.8% and 27.9% higher than the baseline building for the X and Y direction, respectively. On the other hand, the ductility factor sees a notable improvement, as it is 81.9% greater in the X direction and 98.2% in the Y direction. These improvements are the result of the distribution of strength in the optimized building, which has stronger and more ductile columns and beams at its lower floors, allowing it to withstand larger shear forces and having a higher deformation capacity. Although establishing a relationship between optimizing the first mode frequency and the improvement in the building’s Ω_0 and μ would be useful, it would require analyzing a larger sample of buildings and it is out of the scope of this article.

Table 2 – Pushover Results

Building	Pushover X		Pushover Y	
	Ω_0	μ	Ω_0	μ
Optimized	4.00	11.5	3.58	14.07
Traditional	3.23	6.33	2.8	7.1

The performance improvement shown in the pushover is confirmed using nonlinear response history Analysis. The drift responses in figure 4, where it can be seen that for both directions, for a scale factor of 1.0, the optimized building has a significant reduction in the interstory drift for the first five stories, with moderate improvements in the sixth and seventh; nonetheless, this comes at the expense of having a bigger interstory drift in the top three stories. In practice, this means that there is a shift in the expected location of the damage; the optimized building is expected to have more damage in the top stories, as opposed to the baseline building where it is expected to take place in the intermediate stories.

When we increase the scale factor to 2.2 we start to see some differences between the performance in the X and the Y directions. In the X direction the behavior is similar to the previous one for a scale factor of 1.0 with a notable reduction in the interstory drift for the first half of the building that comes at the expense of having larger drifts in the upper stories. On the other hand, the performance in the Y direction shows significant reductions for the optimized building in the interstory drift for the first seven stories, and even though the interstory drift in stories 8 to 10 is larger than in the baseline, these differences are significantly smaller than the ones seen downwards in the building.



Finally, when we increase the scale factor to 3.5 in figure 4 the differences between the two buildings become even clearer, especially in the bottom stories. In the X direction, the first four stories in the baseline structure have interstory drifts close to 10%; meanwhile, in the optimized building, all these stories have interstory drifts smaller than 6%, with the first floor having almost a third of its baseline counterpart. In the Y direction, the first five floors in the traditional building have an interstory drift around 20%, meanwhile in the optimized building, this value goes from 3.5% in the first floor, up to 5.5% in the fifth.

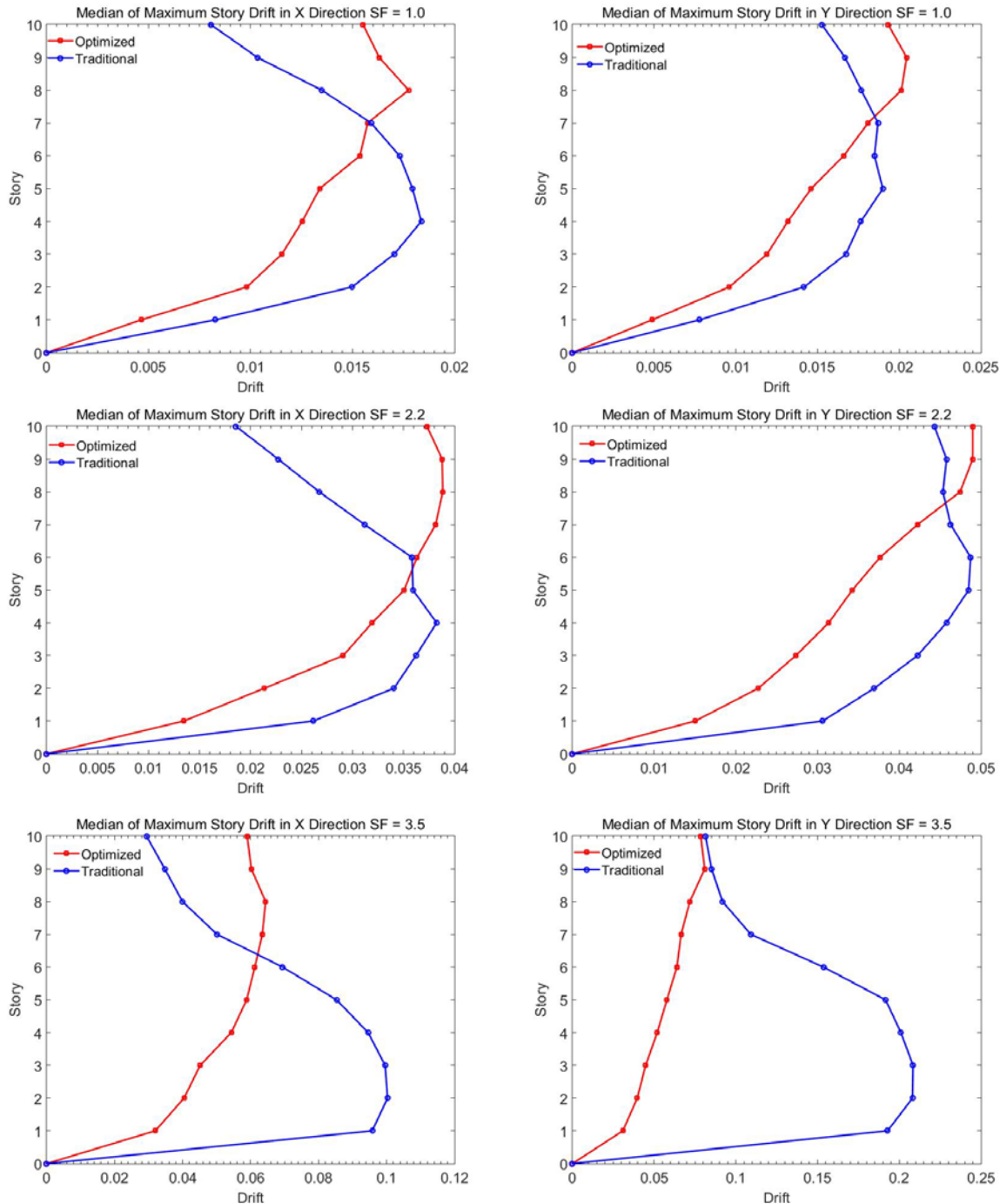


Figure 4 – Median of maximum story drift during nonlinear response history analyses



The observed changes in the structural performance are worthy tradeoffs for a building is preferable to have damage in upper floors than have it in the bottom of the building, as the latter can compromise the structural stability and it is more prone to cause undesirable consequences.

5. Conclusions

A structural optimization method to determine the optimal dimensions of columns in RC Moment Resisting Frames has been proposed. The method is based on a strong mathematical theory that allows to propose an algorithm that is stable and has outstanding numerical efficiency, making the theory building feasible to be run on a consumer-level laptop and achieve results within minutes. The proposed method provides a computationally efficient alternative to significantly improve the seismic performance of RC buildings without incurring in additional costs of materials.

The advantages of the method were exemplified using a 10-story RC building. The seismic performance of the optimized building was compared with a traditional one using 2D fiber models, which were subjected to a Pushover Analysis and to Nonlinear Time History Analyses using the ground motion suite of the FEMA P695 for three different scale factors. The structural analysis revealed that the seismic performance of the optimized building is significantly improved when compared to the traditional one. The Pushover results show that the optimized building comes with an average 26% greater overstrength and a 90% increase on its ductility, two important predictors of the seismic behavior.

The results of the nonlinear response history analyses show that the optimized building has an interstory drift which is significantly smaller in the optimized building for the first six stories, regardless of the scale factor considered, nonetheless, the difference becomes larger as it is increased. Even though the top three floors have smaller interstory drifts in the traditional building, these differences decrease as the scale factor increases. This behavior is preferable to the traditional, as the damage in the lower stories is significantly reduced, especially with the stronger ground motions represented with larger scale factors. In addition to the above, achieving these improvements requires no additional investment in material cost, as both buildings have the same amount of concrete and steel. More supervision would be needed to ascertain that the correct dimensions of columns and beams are used at the prescribed story, nonetheless, the benefits in seismic performance do compensate this endeavor.

7. Copyrights

16WCEE-IAEE 2016 reserves the copyright for the published proceedings. Authors will have the right to use content of the published paper in part or in full for their own work. Authors who use previously published data and illustrations must acknowledge the source in the figure captions.

8. References

- [1] M. Fragiadakis, N. D. Lagaros, An overview to structural seismic design optimisation frameworks, *Computers & Structures* 89 (11) (2011) 1155–1165.
- [2] X. Zou, C. Chan, G. Li, Q. Wang, Multiobjective optimization for performance-based design of reinforced concrete frames, *Journal of structural engineering* 133 (10) (2007) 1462–1474.
- [3] L. H. Li, G., X. Liu, A hybrid simulated annealing and optimality criteria method for optimum design of rc buildings, *Structural Engineering and Mechanics* 35 (1) (2010) 19–35.
- [4] G. Li, H. Lu, X. Liu, A hybrid genetic algorithm and optimality criteria method for optimum design of rc tall buildings under multi-load cases, *The Structural Design of Tall and Special Buildings* 19 (6) (2010) 656–678.



- [5] M. Khatibinia, E. Salajegheh, J. Salajegheh, M. Fadaee, Reliabilitybased design optimization of reinforced concrete structures including soil–structure interaction using a discrete gravitational search algorithm and a proposed metamodel, *Engineering Optimization* 45 (10) (2013) 1147–1165.
- [6] H. S. Park, E. Kwon, Y. Kim, S. W. Choi, Resizing technique-based hybrid genetic algorithm for optimal drift design of multistory steel frame buildings, *Mathematical Problems in Engineering* 2014.
- [7] E. W. Ho
of taller buildings, *Journal of Structural Engineering* 140 (8). ffman, P. W.
- [8] A. E. Zacharenaki, M. Fragiadakis, M. Papadrakakis, Reliability-based optimum seismic design of structures using simplified performance estimation methods, *Engineering Structures* 52 (2013) 707–717.
- [9] M. P. Bendsoe, O. Sigmund, *Topology optimization: theory, methods and applications*, Springer, 2003.
- [10] G. Allaire, *Shape optimization by the homogenization method*, Vol. 146, Springer, 2002.
- [11] P. G. Ciarlet, *Three-dimensional elasticity*, Vol. 1, Elsevier, 1988.
- 21
- [12] J. Sokolowski, A. Zochowski, Topological derivative in shape optimization topological derivative in shape optimization, in: *Encyclopedia of Optimization*, Springer, 2009, pp. 3908–3918.
- [13] L. Tartar, The general theory of homogenization: a personalized introduction, Vol. 7, Springer, 2009.
- [14] F. Murat, L. Tartar, *Calculus of variations and homogenization*, in: *Topics in the mathematical modelling of composite materials*, Springer, 1997, pp. 139–173.
- [15] G. Allaire, S. Aubry, F. Jouve, Eigenfrequency optimization in optimal design, *Computer Methods in Applied Mechanics and Engineering* 190 (28) (2001) 3565–3579.
- [16] A. C. I. A. C. 318), Building code requirements for structural concrete (aci 318-11) and commentary (318r-11), American Concrete Institute Farmington Hills, MI, 2011.
- [17] F. Hecht, New development in freefem++, *Journal of Numerical Mathematics* 20 (3-4) (2012) 251–266.
- [18] S. Mazzoni, F. McKenna, M. H. Scott, G. L. Fenves, et al., *Opensees command language manual*, Pacific Earthquake Engineering Research (PEER) Center.
- [19] U. S. F. E. M. Administration, *Quantification of Building Seismic Performance Factors*, FEMA P695/ June 2009, 2009.
- [20] J. Coleman, E. Spacone, Localization issues in force-based frame elements, *Journal of Structural Engineering* 127 (11) (2001) 1257–1265.